

Article

# Early Detection of Parkinson's Disease Using Fusion of Discrete Wavelet Transformation and Histograms of Oriented Gradients

Himanish Shekhar Das <sup>1</sup>, Akalpita Das <sup>2</sup>, Anupal Neog <sup>3</sup>, Saurav Mallik <sup>4,5,6</sup>, Kangkana Bora <sup>1</sup>  
and Zhongming Zhao <sup>4,7,\*</sup>

- <sup>1</sup> Department of Computer Science and Information Technology, Cotton University, Guwahati 781001, India  
<sup>2</sup> Department of Computer Science and Engineering, GMT Guwahati, Guwahati 781017, India  
<sup>3</sup> Department of AI & Machine Learning COE, IQVIA, Bengaluru 560103, India  
<sup>4</sup> Center for Precision Health, School of Biomedical Informatics, The University of Texas Health Science Center at Houston, Houston, TX 77030, USA  
<sup>5</sup> Department of Environmental Health, Harvard T H Chan School of Public Health, Boston, MA 02115, USA  
<sup>6</sup> Department of Pharmacology and Toxicology, University of Arizona, Tucson, AZ 85724, USA  
<sup>7</sup> Department of Pathology and Laboratory Medicine, McGovern Medical School, The University of Texas Health Science Center at Houston, Houston, TX 77030, USA  
\* Correspondence: zhongming.zhao@uth.tmc.edu; Tel.: +1-713-500-3631

**Abstract:** Parkinson's disease primarily affects people in their later years, and there is no cure for this disease; however, the proper medication of patients can lead to a healthy life. Appropriate care and treatment of Parkinson's disease can be improved if the disease is detected in its early phase. Thus, there is an urgent need to develop novel methods for early illness detection. With this aim for the early detection of Parkinson's disease, in this study, we utilized hand-drawn images by Parkinson's disease patients to effectively reduce the clinical experimental costs for poor people. Initially, discrete wavelet coefficients were extracted for each pattern of images; thereafter, on top of that, histograms of oriented gradient features were also extracted to refine the level of features. Thereafter, the fusion approach-based features were fed to various machine learning algorithms. The proposed work was validated on two different datasets, each of which consisted of various patterns, including spiral, wave, cube, and triangle images. The main contribution of this work is the fusion of two feature extraction techniques, which are histograms of oriented gradient features and discrete wavelet transform coefficients. The extracted features were then provided as input into different machine learning algorithms. In our experiment(s) on two datasets, the results achieved an accuracy of 79.7% and 97.8%, respectively, for all four discrete wavelet transform coefficients. This work demonstrates the utilities of fusion-based features for all four discrete wavelet transformation coefficients to detect Parkinson's disease, using image processing and machine learning techniques.



**Citation:** Das, H.S.; Das, A.; Neog, A.; Mallik, S.; Bora, K.; Zhao, Z. Early Detection of Parkinson's Disease Using Fusion of Discrete Wavelet Transformation and Histograms of Oriented Gradients. *Mathematics* **2022**, *10*, 4218. <https://doi.org/10.3390/math10224218>

Academic Editor: Giancarlo Consolo

Received: 1 October 2022

Accepted: 8 November 2022

Published: 11 November 2022

**Publisher's Note:** MDPI stays neutral with regard to jurisdictional claims in published maps and institutional affiliations.

**Keywords:** Parkinson's disease; image analysis; histogram of oriented gradients; discrete wavelet transformation; machine learning algorithms

**MSC:** 68T01; 68T10; 68T45



**Copyright:** © 2022 by the authors. Licensee MDPI, Basel, Switzerland. This article is an open access article distributed under the terms and conditions of the Creative Commons Attribution (CC BY) license (<https://creativecommons.org/licenses/by/4.0/>).

## 1. Introduction

Parkinson's disease (PD) is the second most common age-related neurodegenerative disease only after Alzheimer's disease. It occurs when people get older. It affects their nervous system, causing them to tremble and stiffen, and resulting in difficulty in walking, standing, and organizing their actions [1]. It also has an impact on the voice and causes other cognitive issues. Both motor and non-motor signs are present in Parkinson's disease. Motor symptoms include tremors, slowness of movement due to muscle stiffness, gait issues, and speech difficulties. Non-motor symptoms, on the other hand, include sleep, mood, and cognitive disorders, such as memory loss, sleep difficulties, and impaired abstract

thought, problem-solving, vocabulary, and visual emotional capacities. The disease is caused by the degeneration of a brain area called the “substantia nigra” in the thalamic region. The dopamine hormone, a synaptic information-relaying neurotransmitter, is in charge of brain and body coordination. PD is characterized by a decrease in dopamine hormone production, which impairs brain–body coordination.

Because there is no treatment for Parkinson’s disease unless it is discovered early, numerous researchers have been working in this sector for the past few years to develop a method for early detection. Utilizing the PD dataset from the University of California-Irvine’s (UCI) deep learning database of speech signals, M. Hariharan et al. developed a hybrid approach for identifying PD using three supervised classifiers. Least squares support vector machines, probabilistic neural networks, and general regression neural networks were the classifiers used in [2]. Using a combination of feature pre-processing approaches, such as Gaussian mixture modelling (GMM), and efficient feature reduction/selection methods, such as principal component analysis (PCA) and linear discriminant analysis, the Parkinson’s dataset achieved a cumulative classification accuracy of 100%. With an accuracy of 97.57%, Satyabrata et al. used voice data to distinguish the PD population from the control group, utilizing feature sets based on PCA and a non-linear-based classification approach [3]. Peker et al. utilized a hybrid model to achieve 98.25% accuracy, selecting features based on minimal redundancy maximum significance (mRMR) and putting them into a complex-valued artificial neural network [4].

Hand tremor is the most frequent symptom used by PD patients to detect the disorder from hand-drawn images/sketches/handwriting, along with many of the other symptoms of Parkinson’s disease. A lot of study has been conducted in the last several years to classify PD using handwriting and hand-drawn pictures. Drotár et al. [5] used the PaHaW Parkinson’s disease handwriting database, which comprised 37 PD patients and 38 healthy persons who completed eight different handwriting tasks, such as drawing an Archimedean spiral and orthographically writing basic syllables, phrases, and sentences. This study used three classifiers—k-nearest neighbor (KNN), support vector machine (SVM), and AdaBoost—to predict PD using conventional kinematic and handwriting pressure data, with an accuracy of 81.3%. Loconsole et al. [6] investigated a novel method for integrating ElectroMyoGraphy data with machine vision algorithms, such as morphological operators and image segmentation. In this investigation, the accuracy of ANN was 95.81% and 95.52%, respectively, for two different situations (dataset 1 with two dynamic and two static characteristics and dataset 2 with only two dynamic features). Using data from a pen with several sensors, Pereira et al. [7] used a convolutional neural network (CNN) to discriminate between PD patients and stable patients. Spiral and meander designs generated by both PD and healthy people made up the findings. Folador et al. [8] employed the histogram of oriented gradients (HOG) descriptor in conjunction with a random forest classifier to accurately distinguish between persons with Parkinson’s disease and those who are healthy. In our previous work, Das et al. [9] evaluated the performance of different machine learning algorithms, using only the features extracted from HOG descriptors for hand-drawn images.

This paper proposes an efficient hybrid fusion-based approach for the early detection of Parkinson’s disease using hand-drawn images. The goal of this work was to use hand-drawn artworks to detect Parkinson’s disease patients, using the fusion of discrete wavelet transform (DWT) coefficients and HOG features, and several classification techniques were utilized to test the efficacy of the proposed model. HOG features are widely used in computer vision tasks for object detection. The HOG descriptor focuses on the structure or the shape of an object. The working dataset consisted of spiral and wave images, where investigation requires not only edge features, but also edge direction, which can be extracted by the HOG descriptor only using the gradients in both the x and y directions. Wavelet transforms are useful for image processing to accurately analyze the abrupt changes in the image that localize means in time and frequency. Wavelets exist for a finite duration, and they have different sizes and shapes. This work also evaluated the performance of various

classifiers, using a variety of performance metrics, such as accuracy, precision, specificity, sensitivity, and F-score. The main contribution of this paper lies in the following aspects:

- The main focus is on the early detection of Parkinson's disease with the help of hand-drawn images, which will reduce the high cost of laboratory examinations and will be useful for poor people who cannot bear the extreme cost of clinical examinations.
- In continuation from our earlier work, in this work, along with HOG features, DWT coefficients were also explored, and a fusion strategy of feature refinement was exploited.
- The proposed models were evaluated on two different datasets composed of various types of patterns.
- The targets were to first identify which type of image was more useful, the impact of higher number of images, which dataset gave better results, and which classification technique would be more useful for this work.

This study is structured as follows: Section 2 explains the database along with the proposed mechanism. Section 3 explains the experimental results of the proposed model, followed by the discussion in Section 4. Finally, the conclusion of the paper is presented in Section 5.

## 2. Materials and Methods

This section explains the databases that were used for this study. It also briefly describes the proposed model, along with the importance of the features that were extracted, as well as the classification algorithms with their set parameters.

### 2.1. Database Description

Two different datasets were used in this study. There is currently no comprehensive database for Parkinson's disease cases, particularly for various types of drawings created by PD sufferers. As a result, for dataset 1, a publicly accessible collection of data was employed in this study. This dataset may be found in the Kaggle repository. In their work, Zham et al. [10] also validated dataset 1. Dataset 2 was obtained with mutual permission from Bernardo et al. [11] for this study. Dataset 2 was created with the help of grants no. 304315/2017-6 and 430274/2018-1 from the Brazilian National Council for Research and Development (CNPq). There are two sorts of photographs in dataset 2. One type of picture is dilated pictures, which include both dilated and processed skeletal pictures. The comprehensive description of both datasets can be found in Table 1. Figure 1 shows examples of photos from both datasets.

**Table 1.** Summary of the two datasets.

Subject	Dataset 1		Dataset 2		
	Spiral	Wave	Spiral	Cube	Triangle
Parkinson	51	51	54	54	58
Healthy	51	51	54	54	58

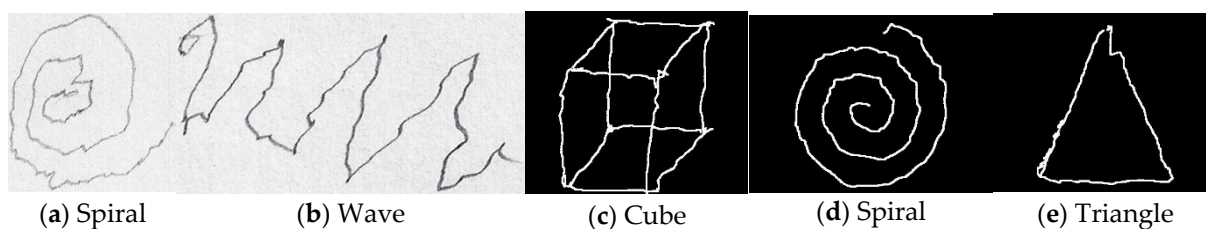


**Figure 1.** Sample images of Parkinson's disease patients (a,b) from dataset 1 and (c–e) from dataset 2.

## 2.2. Proposed Methodology

In this paper, images of various shapes were utilized to verify which shape of images is good for recognition, as well as which algorithm is suitable for the proposed model with higher accuracy for the two different datasets. Initially, single-level 2-D discrete wavelet transform was applied on the input images. It returned the horizontal, vertical, and diagonal detail coefficients' matrices, as well as the approximation coefficient matrix. These coefficients were extracted using the Haar wavelet. On top of each coefficient-based image, HOG features were extracted. The extracted features were then fed into various machine learning algorithms for classification. A comparison was performed to verify the effect of these coefficients. Two types of experiments were performed in this paper. One was with the approximation coefficient with HOG-based features, and another was the combination of all four DWT coefficient-based HOG features. These experiments were performed for the KNN, random forest (RF), SVM, Naïve Bayes (NB), and multilayer perceptron (MLP) algorithms. The aim of this work was to utilize the hand-drawn images from the PD patients and to find out which shape of images is effective to achieve the highest accuracy. Figure 2 gives a clear overview of the proposed methodology.

### 2.2.1. Feature Extraction

- Histogram of oriented gradients

Various variations of attributes and classifiers may be used to recognize an image in a photograph. Several common feature forms have been identified in the literature, including Haar wavelets [12,13] and Gabor filter outputs [14], which are both primarily concerned with appearance; edge templates [15], HOG [16,17], and edgelets [18], which are both primarily concerned with appearance; and shapelets [19], which are all primarily concerned with structure. Shape and form methods are appealing, since they just use one image and can identify both moving and stationary objects. Shape-based applications are thought to have a stronger discriminative impact than appearance-based characteristics. The HOG approach's shape-based algorithms are among the most accurate for visual classification issues in the domain of shape-based algorithms. HOG has been coupled with color characteristics and explicit form templates to identify any item despite the presence of multiple occlusions, proving the ability to recognize objects despite the presence of multiple occlusions.

In this work, we only employed the HOG feature set to extract crucial information from hand-drawn pictures. The use of vision-based algorithms to analyze the orientation of spiral, wave, cube, and triangle forms in photos was suggested [12–14], which we focused on in this work. According to the concept by Dalal and Triggs [16], the detector generates a binary output, indicating if a specific region of an image includes an instance of the targeted item (in our case, various shapes of images). Each picture input into the detector is first converted to a set of spatially discretized gradients. A sub-image of a certain size is taken from this gradient histogram and converted into a function vector (the HOG). This feature vector is then put into a number of machine learning algorithms, which recognize and classify the item as being drawn by a healthy individual or a diseased patient. The major contribution of this work is a detailed investigation of how a set of HOG-based classifiers may be used to determine whether a person has Parkinson's disease. Figure 3 shows the HOG descriptor for spiral and wave images from dataset 1.

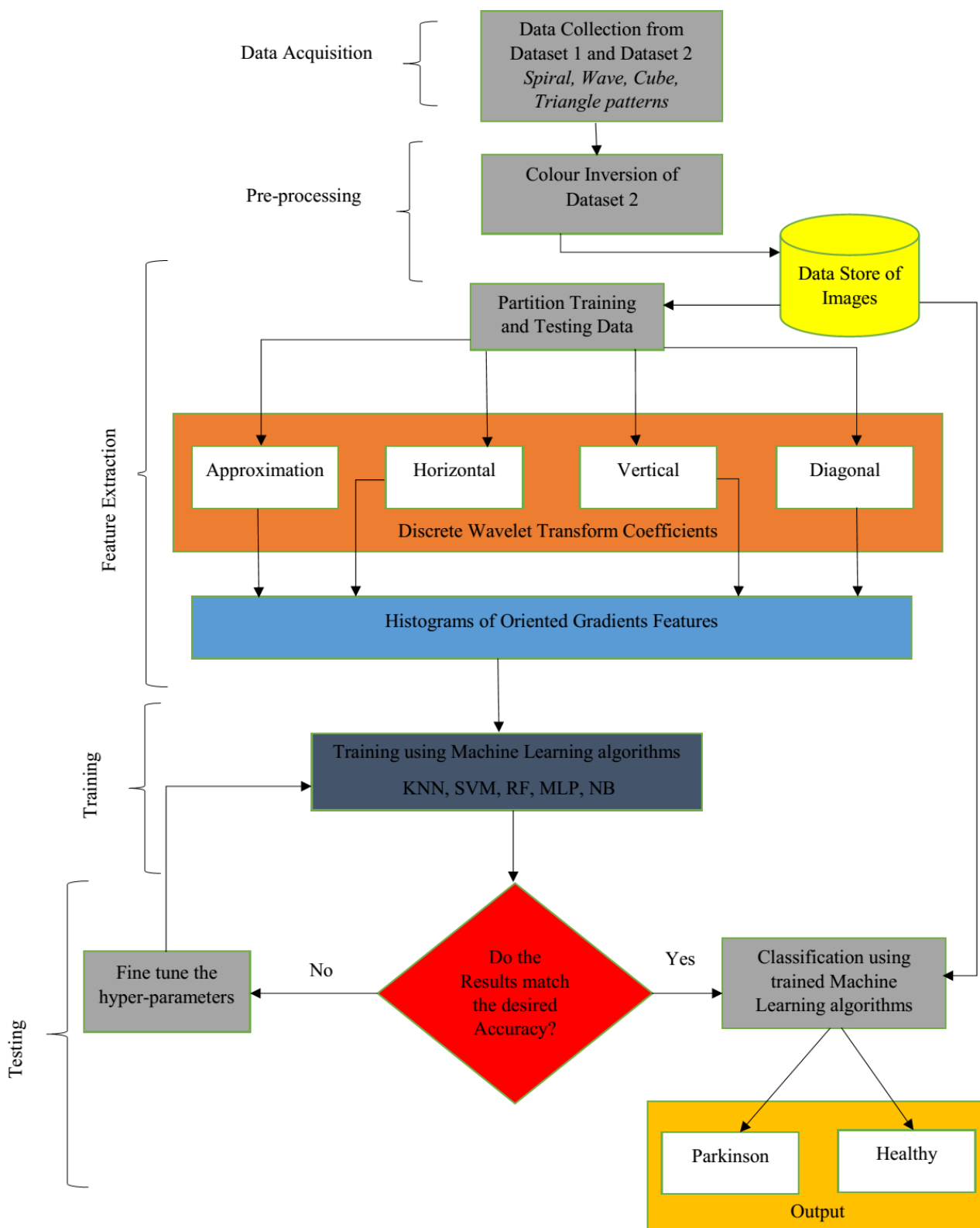
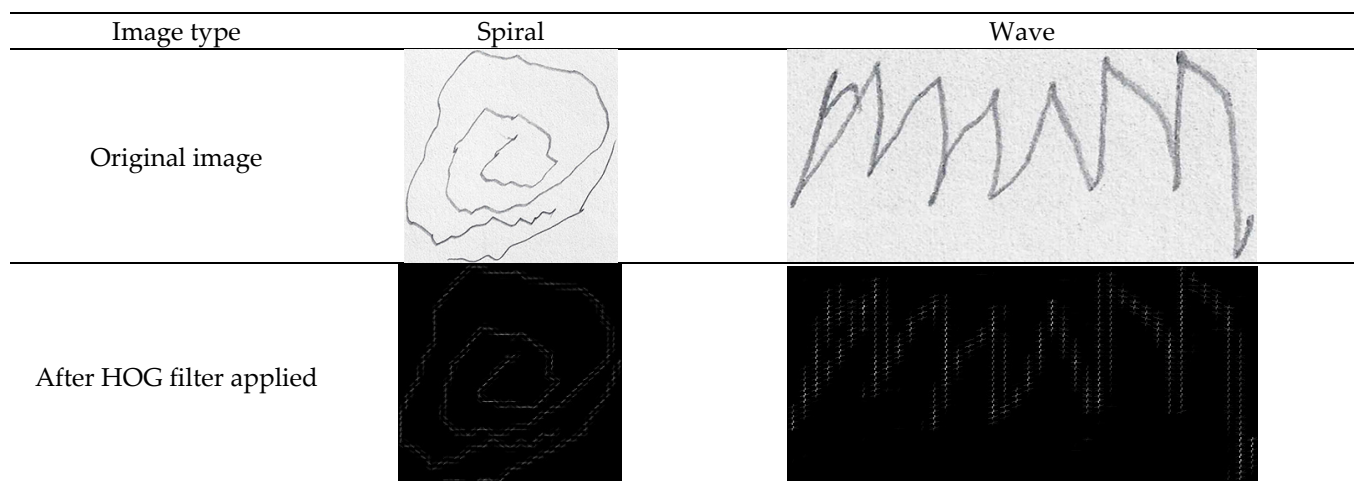


Figure 2. Proposed model for Parkinson's disease detection.



**Figure 3.** HOG descriptor of spiral and wave images.

- Discrete wavelet transform (DWT) coefficients

In signal processing applications such as picture watermarking, the DWT has sparked a lot of attention. The DWT was inspired by multiresolution analysis, which entails dividing an image into frequency channels with constant bandwidth on a logarithmic scale. It has benefits such as a comparable data structure in terms of resolution and deconstruction at every level. The DWT can be utilized as a multistage transformation. An image is divided into four sub-bands at level 1 in the DWT domain, labelled LL, LH, HL, and HH, where LH, HL, and HH represent the finest scale wavelet coefficients, while LL represents the coarse-level coefficients. The LL sub-band can be decomposed to obtain a higher degree of decomposition. On the LL sub-band, the decomposition process continues until the application's intended number of levels is attained. Because human eyes are significantly more sensitive to the low-frequency component, the watermark can be placed in the other three sub-bands to maintain superior picture quality (the LL sub-band).

On the different types of input images, the DWT transformation was applied. Approximation and detailed reconstruction wavelet coefficients were the outputs of these transformations. The Haar wavelet was used as the mother wavelet to recreate the coefficients. The approximation output was the input signal component's low-frequency material, as well as the multidimensional output, which provides high-frequency components, including horizontal, vertical, and diagonal components. These bands are often referred to as low-low (LL), low-high (LH), high-low (HL), and high-high (HH). The HOG feature descriptor counted the number of times a gradient orientation occurred in a specific area of an image. It calculated the gradient orientation of each of the decomposed images' small square regions. Figure 4 depicts all DWT coefficients from Figure 4a–d and their HOG representations from Figure 4e–h for a spiral image from dataset 1.

### 2.2.2. Classification Algorithms for Evaluation

To validate the performance of the suggested model and to determine which type of image is best for achieving the maximum accuracy, a variety of machine learning algorithms were used. The following are the settings for various simulation approaches. For KNN, the value of K was set to 2, while the number of trees in the forest was set to 100 for RF. The regularization parameter was set to 0.025 and the kernel function to "linear" for SVM. The hidden layer size for the MLP network was set to 100, the activation to "relu", the weight optimization to "adam", the alpha value to 1, the learning rate to 0.001, the maximum number of iterations to 1000, and the epsilon value to  $1 \times 10^{-8}$ . For the experiment, default values for NB were taken into account.

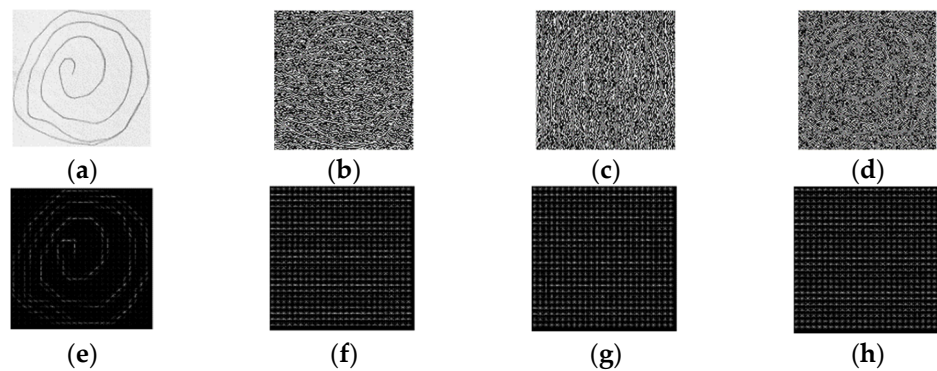


Figure 4. DWT coefficients (a–d) and HOG features (e–h) of a spiral image.

### 3. Results

To confirm the efficacy of each picture form, the proposed experimental investigation was conducted in two phases. Comparable images from many categories, such as spiral, wave, triangle, and cube, were trained and assessed in the first phase. The model was then evaluated using a random figure in the second stage, which used a combination of various categories of images from the relevant dataset in the training phase.

For the classification task, we used the following metrics to check the performance of each classifier. From the confusion matrix, we obtained the following parameters: (a) true positives (TP), (b) false negatives (FN), (c) true negatives (TN), and (d) false positives (FP). Table 2 shows the various performance metrics evaluated to check the efficiency of the proposed model in this work.

Table 2. Assessment of performance measures.

Performance Metrics	Formulae
Accuracy	$\frac{True\ Positive + True\ Negative}{True\ Positive + True\ Negative + False\ Positive + False\ Negative}$
Sensitivity	$\frac{True\ Positive}{True\ Positive + False\ Negative}$
Specificity	$\frac{True\ Negative}{True\ Negative + False\ Positive}$
Precision	$\frac{True\ Positive}{True\ Positive + False\ Positive}$
F-score	$\frac{(2 * Precision * Sensitivity)}{(Precision + Sensitivity)}$

#### 3.1. Using Only Approximation Coefficient of DWT with HOG

##### 3.1.1. Dataset 1

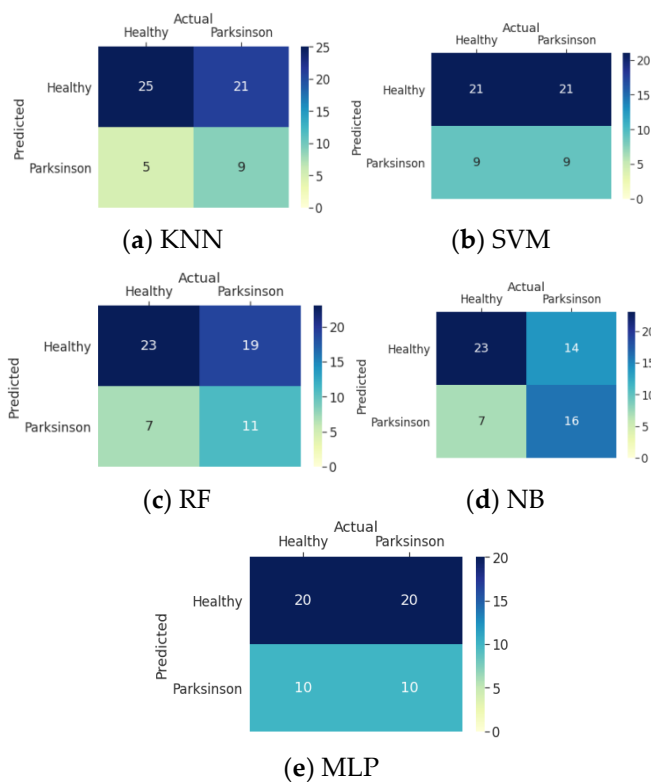
Tables 3–7 contain the result sets for spiral and wave images, as well as a mixture of spiral and wave images, from when HOG features were extracted from only the approximation coefficient. From Tables 3 and 4 of spiral and wave images, the spiral images showed a maximum possible recognition rate of 81.3%, and from Figures 5 and 6, it can be seen that the overall RF algorithm gave the most accurate result, with an accuracy of 78.9%.

Table 3. Results of five machine learning algorithms using spiral images.

	KNN (%)	SVM (%)	RF (%)	MLP (%)	NB (%)
Accuracy	73.3	76.7	81.3	73.3	56.7
Sensitivity	80.0	80.0	70.7	73.3	86.7
Specificity	66.7	73.3	85.3	73.3	26.7
Precision	70.6	75.0	83.1	73.3	54.2
F-score	75.0	77.4	76.3	73.3	66.7

**Table 4.** Results of five machine learning algorithms using wave images.

	KNN (%)	SVM (%)	RF (%)	MLP (%)	NB (%)
Accuracy	80.0	70.0	80.3	66.7	43.3
Sensitivity	86.7	73.3	86.7	66.7	40.0
Specificity	73.3	66.7	62.7	66.7	46.7
Precision	76.5	68.8	68.4	66.7	42.9
F-score	81.3	71.0	76.5	66.7	41.4



**Figure 5.** Confusion matrices (a–e) for approximation coefficient from dataset 1.

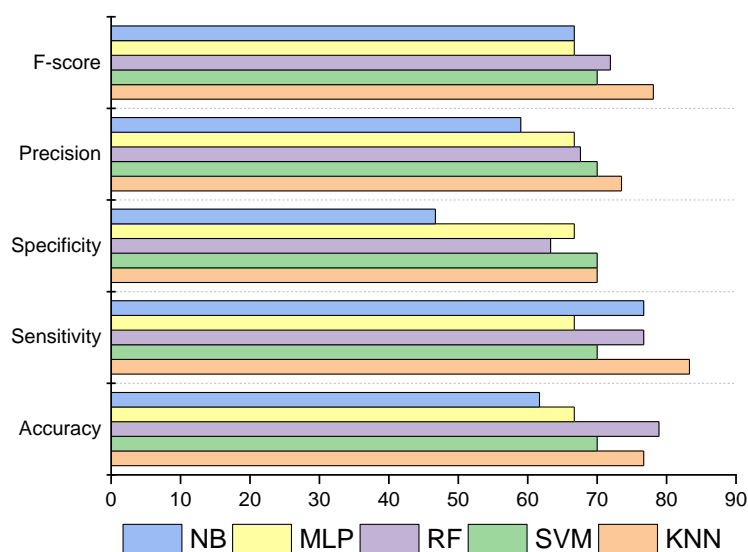


**Figure 6.** Performance summary of dataset 1 (%).

**Table 5.** Results of five machine learning algorithms using spiral images.

	KNN (%)	SVM (%)	RF (%)	MLP (%)	NB (%)
Accuracy	79.2	95.8	87.5	95.8	87.5
Sensitivity	100	100	100	100	83.3
Specificity	16.7	83.3	50.0	83.3	100
Precision	78.2	94.7	85.7	94.7	100
F-score	87.8	97.3	92.3	97.3	90.9

**Table 6.** Results of five machine learning algorithms using cube images.

	KNN (%)	SVM (%)	RF (%)	MLP (%)	NB (%)
Accuracy	100	100	100	100	100
Sensitivity	100	100	100	100	100
Specificity	100	100	100	100	100
Precision	100	100	100	100	100
F-score	100	100	100	100	100

**Table 7.** Results of five machine learning algorithms using triangle images.

	KNN (%)	SVM (%)	RF (%)	MLP (%)	NB (%)
Accuracy	94.8	94.7	91.7	91.7	91.6
Sensitivity	100	100	100	100	100
Specificity	83.3	66.7	73.3	66.7	66.7
Precision	94.7	90.0	91.9	90.0	90.0
F-score	97.3	94.7	95.7	94.7	94.7

3.1.2. Dataset 2

From Tables 5–7, it is clearly visible that, for the approximation coefficient, cube images are the most suitable ones, and from Figures 7 and 8, it can be concluded that overall SVM performed best for dataset 2, with an accuracy of 95.6%.

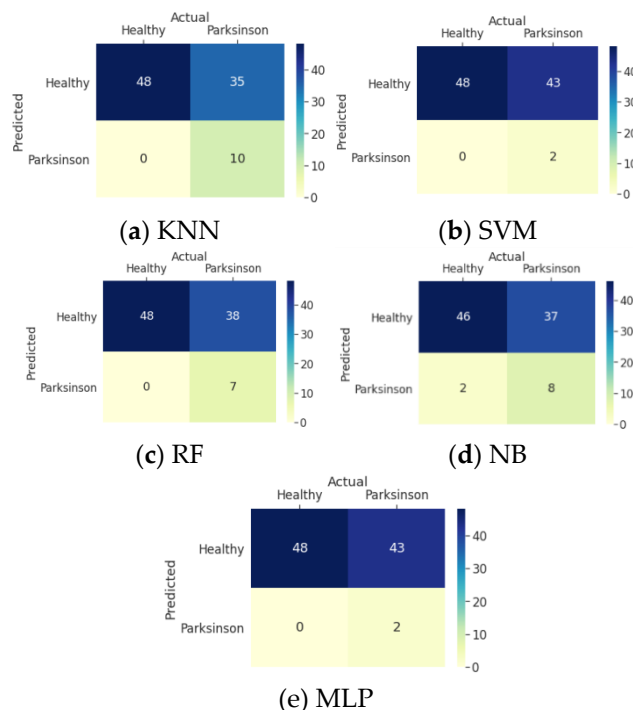


**Figure 7.** Confusion matrices (a–e) for approximation coefficient from dataset 2.

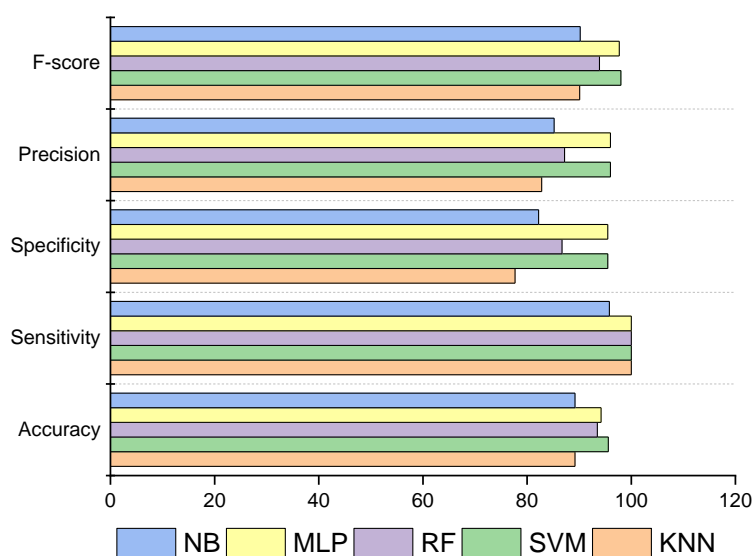


**Figure 8.** Performance summary of dataset 2 (%).

### 3.2. Using All Four DWT Coefficients with HOG

Tables 8–12 contain the result sets for spiral, cube, and triangle images, as well as a mixture of spiral, cube, and triangle images, from when HOG features were extracted from all four DWT coefficients, which are approximation, horizontal, vertical, and diagonal.

#### 3.2.1. Dataset 1

From Tables 8 and 9 of spiral and wave images, the spiral images showed a maximum possible recognition rate of 82.7%, and from Figures 9 and 10, we can conclude that overall RF achieved 79.7% accuracy.

**Table 8.** Results of five machine learning algorithms using spiral images.

	KNN (%)	SVM (%)	RF (%)	MLP (%)	NB (%)
Accuracy	70.0	76.7	82.7	76.7	53.3
Sensitivity	53.3	80.0	73.3	80.0	93.3
Specificity	86.7	73.3	86.7	73.3	13.3
Precision	80.0	75.0	84.6	75.0	51.8
F-score	64.0	77.4	78.6	77.4	66.7

**Table 9.** Results of five machine learning algorithms using wave images.

	KNN (%)	SVM (%)	RF (%)	MLP (%)	NB (%)
Accuracy	73.3	73.3	76.7	73.3	53.3
Sensitivity	60.0	66.7	80.0	66.7	53.3
Specificity	86.7	80.0	73.3	80.0	53.3
Precision	81.8	76.9	75.0	76.9	53.3
F-score	69.2	71.4	77.4	71.4	53.3

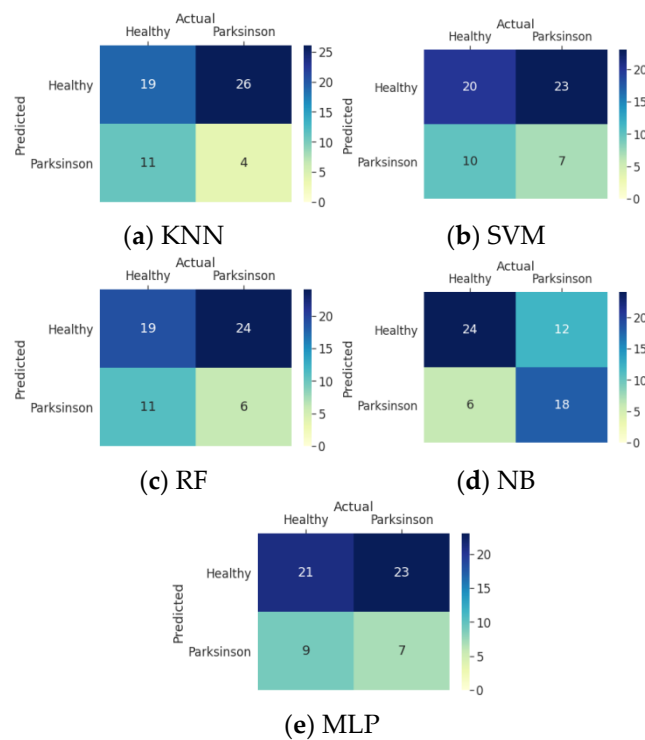


Figure 9. Confusion matrices (a–e) for all DWT coefficients from dataset 1.

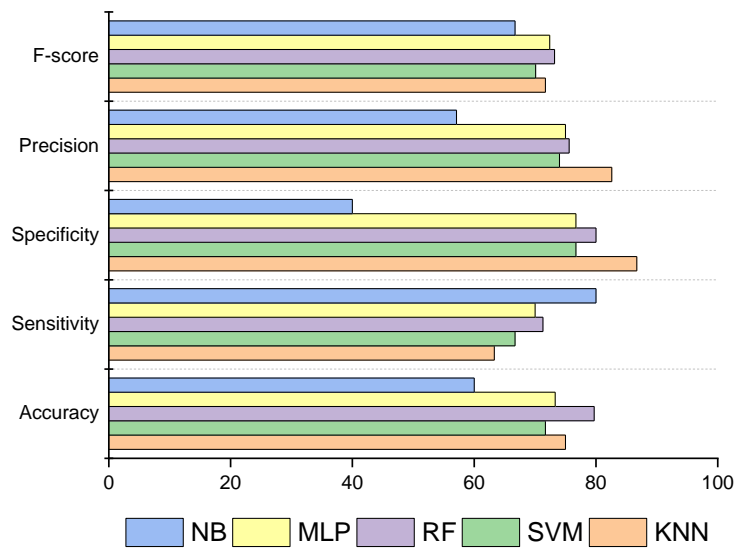


Figure 10. Performance summary of dataset 1 (%).

### 3.2.2. Dataset 2

From Tables 10–12, we can conclude that for all four coefficients, the cube images achieved maximum accuracy, and from Figures 11 and 12, it can be seen that overall SVM achieved an accuracy of 97.8%.

**Table 10.** Results of five machine learning algorithms using spiral images.

	KNN (%)	SVM (%)	RF (%)	MLP (%)	NB (%)
Accuracy	87.5	95.8	95.8	95.8	95.8
Sensitivity	100	100	100	100	100
Specificity	50.0	83.3	83.3	83.3	83.3
Precision	85.7	94.7	94.7	94.7	94.7
F-score	92.3	97.2	97.2	97.2	97.2

**Table 11.** Results of five machine learning algorithms using cube images.

	KNN (%)	SVM (%)	RF (%)	MLP (%)	NB (%)
Accuracy	100	100	100	100	100
Sensitivity	100	100	100	100	100
Specificity	100	100	100	100	100
Precision	100	100	100	100	100
F-score	100	100	100	100	100

**Table 12.** Results of five machine learning algorithms using triangle images.

	KNN (%)	SVM (%)	RF (%)	MLP (%)	NB (%)
Accuracy	95.8	91.7	91.7	91.7	91.7
Sensitivity	100	100	100	100	100
Specificity	83.3	66.7	66.7	66.7	66.7
Precision	94.7	90.0	90.0	90.0	90.0
F-score	97.2	94.7	94.7	94.7	94.7

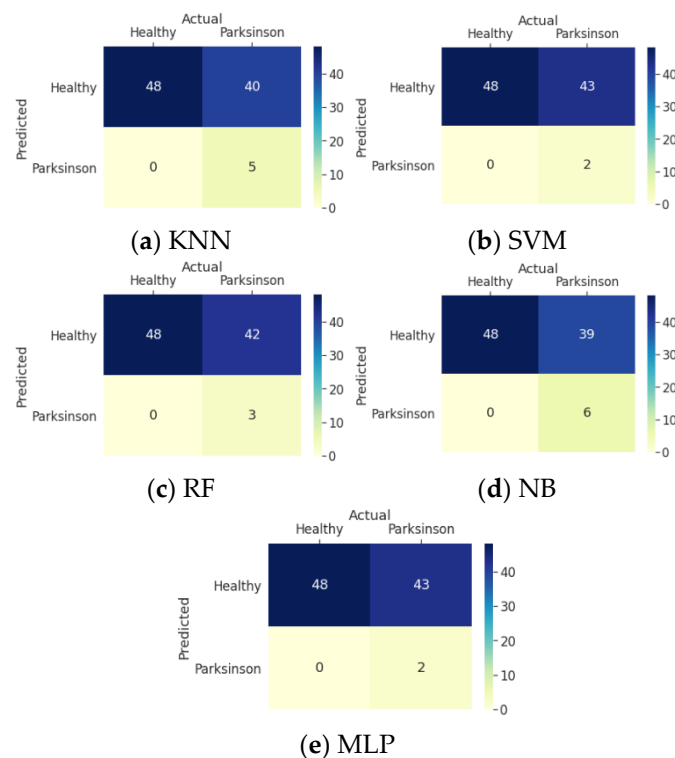


**Figure 11.** Confusion matrices (a–e) for all DWT coefficients from dataset 2.

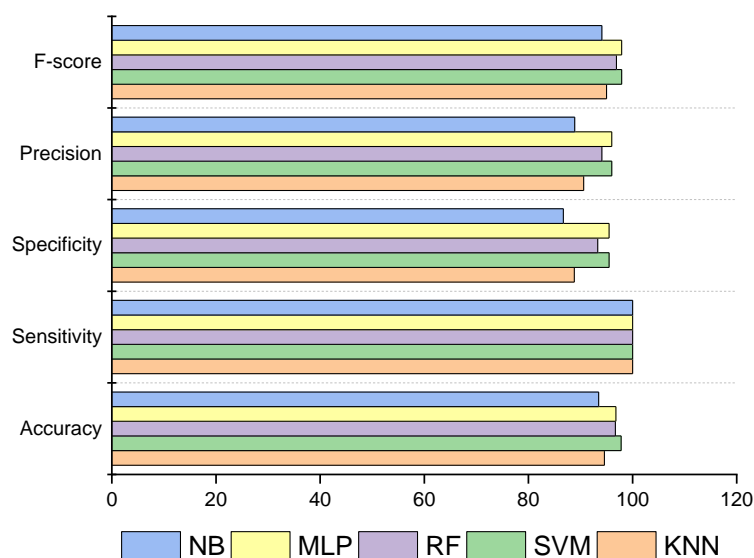


Figure 12. Performance summary of dataset 2 (%).

#### 4. Discussion

From the experimental results, it can be concluded that the fusion-based features surpassed the result obtained using only the approximation coefficient. Folador et al. [8] utilized the HOG descriptor in conjunction with a random forest classifier to accurately distinguish between persons with Parkinson’s disease and those who are healthy. They achieved a highest accuracy, sensitivity, and specificity classification success rates of 83%, 85%, and 81%, respectively. In our previous work [9], we evaluated the performance of different machine learning algorithms using only the features extracted from HOG descriptors for hand-drawn images. It was found that for dataset 1 and dataset 2, the proposed model was able to achieve a highest accuracy of 74.7% and 96.8%, respectively.

To further enhance the previous results, in this work, two different approaches were compared. The key feature of this work is that DWT coefficients were extracted first, and on top of that, HOG features were extracted for feature refinement; thereafter, the extracted features were fed to the different machine learning algorithms. In DWT coefficients, there are also various types of coefficients; therefore, in this work, the efficiency of those coefficients was also evaluated. One experimental approach was to extract using the approximation coefficient, and the other one was with all the four coefficients. An analysis was performed for the approximation coefficient against all coefficients. From the findings, it can be concluded that the second approach outperformed the first approach. Table 13 shows the accuracy performance comparison of the proposed approaches with other state-of-the-art techniques.

Table 13. Comparison of proposed approaches with the state-of-the-art techniques.

Approach	Accuracy (%)
DWT (1 coefficient) + HOG (Proposed) [Dataset 1]	78.90
DWT (4 coefficients) + HOG (Proposed) [Dataset 1]	79.70
DWT (1 coefficient) + HOG (Proposed) [Dataset 2]	95.60
DWT (4 coefficients) + HOG (Proposed) [Dataset 2]	97.80
Folador et al. [8] (2019) [Dataset 1]	83.00
Das et al. [9] (2020) [Dataset 1]	74.70
Das et al. [9] (2020) [Dataset 2]	96.80

## 5. Conclusions

In this work, we adopted a fusion technique, combining discrete wavelet transform coefficients and histograms of oriented gradient features to detect Parkinson's disease from the hand-drawn images drawn by Parkinson's disease-affected patients. It outperformed the same experiment that was performed with only histograms of oriented gradient features. The main purpose of this research was to extract relevant information from discrete wavelet transform coefficients and identify the most important coefficients. In addition, a fusion technique was used to compare the performance of the approach to previous work that exclusively used histograms of oriented gradient characteristics. The results of the experiments show that fusion-based features outperform the outcome produced using merely the approximation coefficient. In our earlier work, we examined the effectiveness of several machine learning techniques for hand-drawn pictures, using just the features retrieved from histograms of oriented gradient descriptors. For datasets 1 and 2, an accuracy of 74.7% and 96.8%, respectively, was attained solely using histograms of oriented gradient features on various machine learning methods. In order to improve on the prior findings, two distinct methodologies were examined in this research. The main characteristic of this work is that discrete wavelet transform coefficients were extracted first, followed by histograms of oriented gradient features for feature refinement, and finally, the extracted features were fed as input to various machine learning methods. There are numerous sorts of coefficients in the discrete wavelet transform; thus, the effectiveness of various coefficients was also investigated in this work. The first method was to extract using only the approximation coefficient, and the second method was to extract using all four coefficients. The approximation coefficient was compared against other discrete wavelet transform coefficients, such as horizontal, vertical, and diagonal. According to the findings of the experiments, the second strategy obtained 76.7% and 97.4% accuracy for dataset 1 and dataset 2, respectively. Another conclusion is that random forest and support vector machine classifiers had the most promising outcomes when compared to other classifiers; out of different kinds of hand-drawn figures, spiral pattern images showed the best performance. The suggested method has a restriction because there is not as much data for the hand-drawn images. With a larger amount of data, the robustness of the proposed models could have been tested. While the experimental results for the small dataset scenario are encouraging, more work can be performed to expand the datasets using augmentation techniques. With more image classes being available, we may develop deep learning models for the better detection of features.

**Author Contributions:** Conceptualization, H.S.D.; data curation, A.N.; formal analysis, H.S.D.; funding acquisition, A.D.; investigation, H.S.D.; methodology, H.S.D.; project administration, A.D.; resources, H.S.D.; software, A.N.; supervision, H.S.D.; validation, H.S.D.; visualization, A.N.; writing—original draft, H.S.D.; writing—review and editing, H.S.D., A.D., Z.Z., S.M. and K.B. All authors have read and agreed to the published version of the manuscript.

**Funding:** This research was funded by the Assam Science and Technology University (ASTU), Guwahati, under the Collaborative Research Scheme of TEQIP-III, grant number ASTU/TEQIP-III/COLLABORATIVE RESEARCH/2019/2479.

**Data Availability Statement:** The datasets used and/or analyzed during the current study are available from the corresponding author upon reasonable request.

**Acknowledgments:** Z.Z. was partially supported by Chair Professorship Fund. The funders did not participate in the study design, data analysis, decision to publish, or preparation of the manuscript.

**Conflicts of Interest:** The authors declare no conflict of interest.

## References

1. Mohamed, G.S. Parkinson's disease diagnosis: Detecting the effect of attributes selection and discretization of Parkinson's disease dataset on the performance of classifier algorithms. *Open Access Libr. J.* **2016**, *3*, 1–11. [[CrossRef](#)]
2. Hariharan, M.; Polat, K.; Sindhu, R. A new hybrid intelligent system for accurate detection of Parkinson's disease. *Comput. Methods Programs Biomed.* **2014**, *113*, 904–913. [[CrossRef](#)] [[PubMed](#)]
3. Aich, S.; Younga, K.; Hui, K.L.; Al-Absi, A.A.; Sain, M. A nonlinear decision tree based classification approach to predict the Parkinson's disease using different feature sets of voice data. In Proceedings of the 2018 20th International Conference on Advanced Communication Technology (ICACT), Chuncheon, Korea, 11–14 February 2018; pp. 638–642.
4. Peker, M.; Sen, B.; Delen, D. Computer-Aided diagnosis of Parkinson's disease using complex-valued neural networks and mRMR feature selection algorithm. *J. Healthc. Eng.* **2015**, *6*, 281–302. [[CrossRef](#)] [[PubMed](#)]
5. Drotár, P.; Mekyska, J.; Rektorová, I.; Masarová, L.; Smékal, Z.; Faundez-Zanuy, M. Evaluation of handwriting kinematics and pressure for differential diagnosis of Parkinson's disease. *Artif. Intell. Med.* **2016**, *67*, 39–46. [[CrossRef](#)] [[PubMed](#)]
6. Loconsole, C.; Trotta, G.F.; Brunetti, A.; Trotta, J.; Schiavone, A.; Tatò, S.I.; Losavio, G.; Bevilacqua, V. Computer vision and EMG-based handwriting analysis for classification in Parkinson's disease. In *International Conference on Intelligent Computing*; Springer: Cham, Switzerland, 2017; pp. 493–503.
7. Pereira, C.R.; Weber, S.A.; Hook, C.; Rosa, G.H.; Papa, J.P. Deep learning-aided Parkinson's disease diagnosis from handwritten dynamics. In Proceedings of the 29th SIBGRAPI Conference on Graphics, Patterns and Images (SIBGRAPI), Sao Paulo, Brazil, 4–7 October 2016; pp. 340–346.
8. Folador, J.P.; Rosebrock, A.; Pereira, A.A.; Vieira, M.F.; de Oliveira Andrade, A. Classification of handwritten drawings of people with Parkinson's disease by using histograms of oriented gradients and the random forest classifier. In *Latin American Conference on Biomedical Engineering*; Springer: Cham, Switzerland, 2019; pp. 334–343.
9. Das, A.; Das, H.S.; Neog, A.; Reddy, B.B.; Swargiary, M. Performance Analysis of Different Machine Learning Classifiers in Detection of Parkinson's Disease from Hand-Drawn Images Using Histogram of Oriented Gradients. In *Applications of Artificial Intelligence in Engineering*; Gao, X.Z., Kumar, R., Srivastava, S., Soni, B.P., Eds.; Springer: Singapore, 2020; pp. 205–215.
10. Zham, P.; Kumar, D.K.; Dabnichki, P.; Poosapadi Arjunan, S.; Raghav, S. Distinguishing different stages of Parkinson's disease using composite index of speed and pen-pressure of sketching a spiral. *Front. Neurol.* **2017**, *8*, 435. [[CrossRef](#)] [[PubMed](#)]
11. Bernardo, L.S.; Quezada, A.; Munoz, R.; Maia, F.M.; Pereira, C.R.; Wu, W.; de Albuquerque, V.H.C. Handwritten pattern recognition for early Parkinson's disease diagnosis. *Pattern Recognit. Lett.* **2019**, *125*, 78–84. [[CrossRef](#)]
12. Papageorgiou, C.; Poggio, T. A trainable system for object detection. *Int. J. Comput. Vis.* **2000**, *38*, 15–33. [[CrossRef](#)]
13. Viola, P.; Jones, M.J.; Snow, D. Detecting pedestrians using patterns of motion and appearance. *Int. J. Comput. Vis.* **2005**, *63*, 153–161. [[CrossRef](#)]
14. Cheng, H.; Zheng, N.; Qin, J. Pedestrian detection using sparse Gabor filter and support vector machine. In Proceedings of the Intelligent Vehicles Symposium, Las Vegas, NV, USA, 6–8 June 2005; pp. 583–587.
15. Gavrila, D.M.; Giebel, J.; Munder, S. Vision-based pedestrian detection: The protector system. In Proceedings of the IEEE Intelligent Vehicles Symposium, Parma, Italy, 14–17 June 2004; pp. 13–18.
16. Dalal, N.; Triggs, B. Histograms of oriented gradients for human detection. In Proceedings of the 2005 IEEE Computer Society Conference on Computer Vision and Pattern Recognition (CVPR'05), San Diego, CA, USA, 20–25 June 2005; Volume 1, pp. 886–893.
17. Zhu, Q.; Yeh, M.C.; Cheng, K.T.; Avidan, S. Fast human detection using a cascade of histograms of oriented gradients. In Proceedings of the 2006 IEEE Computer Society Conference on Computer Vision and Pattern Recognition (CVPR'06), New York, NY, USA, 17–22 June 2006; Volume 2, pp. 1491–1498.
18. Wu, B.; Nevatia, R. Detection of multiple, partially occluded humans in a single image by bayesian combination of edgelet part detectors. In Proceedings of the Tenth IEEE International Conference on Computer Vision (ICCV'05), Beijing, China, 17–21 October 2005; Volume 1, pp. 90–97.
19. Sabzmejdani, P.; Mori, G. Detecting pedestrians by learning shapelet features. In Proceedings of the 2007 IEEE Conference on Computer Vision and Pattern Recognition, Minneapolis, MN, USA, 17–22 June 2007; pp. 1–8.